

Development of New Methods for Position Estimation of Underground Acoustic Source Using a Passive SONAR System

Soon Suck Jarng, Je Hyeong Lee, and Heung Gu Ahn

Abstract : The aim of the work described in this paper is to develop a complex underground acoustic system which detects and localizes the origin of an underground hammering sound using an array of hydrophones located about 100m underground. Three different methods for the sound localization will be presented, a time-delay method, a power-attenuation method and a hybrid method. In the time-delay method, the cross correlation of the signals received from the array of sensors is used to calculate the time delays between those signals. In the power-attenuation method, the powers of the received signals provide a measure of the distances of the source from the sensors. In the hybrid method, both informations of time-delays and power-ratios are coupled together to produce better performance of position estimation. A new acoustic imaging technique has been developed for improving the hybrid method. This new acoustic imaging method shows the multi-dimensional distribution of the normalized cost function, so as to indicate the trend of the minimizing direction toward the source location. For each method the sound localization is carried out in three dimensions underground. The distance between the true and estimated origins of the source is 28m for a search area of radius 250m.

Keywords : SONAR, sensor array, position estimation, underground, time delay, power attenuation, hybrid

I. Introduction

The ability to detect and determine the position of an underground sound source is desirable both for civilian and military purposes, for example, for rescue following collapse of mining tunnels, or for the detection of covert underground operations [1,2,3]. Compared to the similar problem in air or in water there are a number of features which cause additional difficulties - the medium is likely to be inhomogeneous with unknown properties, objects which scatter sound are usually present, and there are practical difficulties in positioning (and moving) the acoustic sensors.

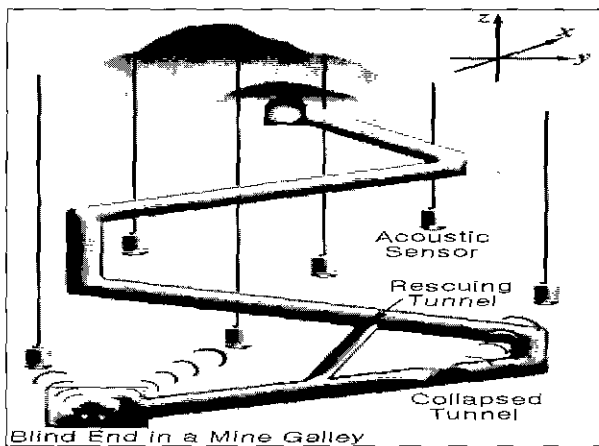


Fig. 1. An underground passive SONAR system for rescue following collapse of mining tunnels.

A suitable acoustic system might consist of a number of acoustic sensors positioned in the suspected locality of the sound source, as shown in Fig. 1. The type of sensor

employed depends on their location. Geophones are velocity-sensitive transducers intended for use at or just below the ground surface. Hydrophones are pressure sensitive and designed to operate in water; they are therefore suitable for locating in water-filled boreholes. The use of such boreholes offers the advantage that the interference from noise caused by activity on the surface is reduced; also, by placing the sensors at various depths a 3-dimensional arrangement can be obtained, more so than with an arrangement on the surface. The maximum operating depth of 300 m for the commonly-used spherical hydrophone [4] is more than adequate for the current application.

In the work reported here, the underground material is granitic beyond a depth of just a few meters. The standard value for the wave propagation velocity in granite is about 6000 m/s [5] but there will be inevitable variations from this in practice, caused by inhomogeneities such as rock faults and rock-soil mixtures. Each hydrophone in the array of sensors will receive acoustic signals from the sound source which have propagated through a medium with uncertain sound speed and unknown attenuation, and possibly along more than one path. The information available is therefore restricted to the detected arrival times and perceived powers of the signal, without assumptions about the sound speed and rate of attenuation [6].

The aim of the work is to develop an underground acoustic system which detects and determines the location of an underground hammering sound, using an array of hydrophones positioned underground. Three algorithms for estimating the location are presented and their predictions are compared with the known location in a particular experiment. A new acoustic imaging method is presented in which the multi-dimensional distribution of the normalized cost function is monitored, so as to indicate the trend of the minimizing direction toward the source location.

II. Experimental arrangement

The general layout of the electro-acoustic system is shown in Fig. 2. Six holes of diameter 150 mm were bored vertically into the ground to depths of between 80 m and 120 m in the vicinity of an existing underground tunnel. After drilling, these boreholes filled with water naturally. A hydrophone, Brüel and Kjør type 8106 [7], was placed at or near the bottom of each hole, with a 150 m watertight low-impedance core cable (B&K AC0101) providing the connection to the surface. To eliminate the 60 Hz ground noise caused by the potential difference between the ground surface and the hydrophone location [8], batteries were used to power all of the components of the system, and the cable to each hydrophone was completely shielded [9].

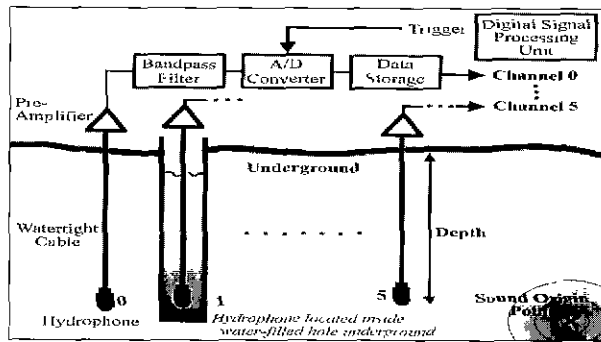


Fig. 2. The overall layout of the underground experimental apparatus.

The output from each hydrophone was amplified by 60 dB for all six channels and then captured by a multi-channel A/D storage unit at a sampling frequency of 10 kHz, using the DT-VEE software package [10]. In parallel with observation of the signals by a battery-operated digital storage oscilloscope, a headphone was used to monitor the sound within the boreholes.

Several locations within the tunnel were selected for the origin of the sound, which was produced by a 10 kg hammer being struck on the tunnel wall.

III. Algorithms for locating the sound source

Three methods have been developed and tested for determining the location of the sound source. The first of these, a time-delay method, uses the differences in the detected arrival times of the sound signal at the hydrophones. The second, a power-attenuation method, uses the information provided by the relative strengths of the signals. The third is a hybrid method in which both the arrival times and signal strengths are used.

In all of the methods the position of the i^{th} hydrophone ($i = 0, 1, \dots, n-1$) is denoted by cartesian coordinates (x_i, y_i, z_i) and the unknown location of the sound source by (x, y, z) . The sound speed v and attenuation α (dB/m) are assumed to be constant, but also unknown. Solutions for x, y, z, v and α are sought by minimising cost functions. Although six hydrophones were used in the experimental work, the methods are not limited to this number and more

could be used to improve the estimating power.

1. Time-delay method

Since the time at which the sound originates is unknown, all times in the problem are relative and one of the hydrophones, label i , is taken as the reference. ΔT_{ij} denotes the time of arrival, or time delay, of the signal at the j^{th} hydrophone relative to its arrival at the i^{th} reference hydrophone. Ideally, $r_j - r_i = \Delta T_{ij} \cdot v$, where $r_i = \sqrt{(x_i - x)^2 + (y_i - y)^2 + (z_i - z)^2}$ is the distance from the sound source to the i^{th} hydrophone. However, variations in v and errors in measuring the arrival times mean that in general it will not be possible to satisfy this equation exactly. Instead, a solution is sought which minimises the sum of the squares of the residuals, given by the function.

$$F_{i,j}(x, y, z, v) = \sum_{j=0, j \neq i}^{n-1} |r_j - r_i - \Delta T_{ij} \cdot v| \quad (1)$$

The time delays, ΔT_{ij} for $j=0, 1, \dots, n-1$, are calculated using unbiased cross-correlation [11] between the signal from each hydrophone and that from the reference. Errors in determining these time delays may be caused by propagation effects and by the presence of other noise sources in the environment.

2. Power-attenuation method

The acoustic waves radiated by the sound source are assumed to be attenuated geometrically according to the inverse square of distance and by the medium at a rate of α dB/m, so that the intensity at distance r is given by

$$I(r) = I_0 \cdot \left(\frac{1}{r}\right)^2 \cdot 10^{-\alpha(1-r)} \quad (2)$$

where I_0 is the intensity at 1 m from the source [12]. The material attenuation coefficient, α , is unknown but is assumed to be constant.

The recorded signals consist of samples of discrete pressures $P(k)$, $k = -N+1, \dots, -1, 0, 1, \dots, N-1$. If P_{S+N} denotes a sample containing the signal from the sound source together with background noise, and P_N a sample of background noise only, then the time-averaged acoustic intensity of the signal from the sound source can be calculated using

$$\varepsilon I = \frac{1}{N} \sum_{k=0}^{N-1} P_{S+N}^2(k) - \frac{1}{N} \sum_{k=0}^{N-1} P_N^2(k) \quad (3)$$

where ε is a constant, equal to $\rho_0 v$ for a plane wave. The power ratio ΔP_{ij} of the j^{th} hydrophone relative to the i^{th} reference hydrophone is defined as $I(r_j)/I(r_i)$. According to the attenuation formula of Eq. (2) this ratio theoretically should equal $(r_i^2/r_j^2)10^{-\alpha(r_i-r_j)}$. The cost function to be minimised is therefore

$$F_{i,j}(x, y, z, \alpha) = \sum_{j=0, j \neq i}^{n-1} \left| \Delta P_{ij} - \left(\frac{r_i}{r_j}\right)^2 \cdot 10^{-\alpha(r_i-r_j)} \right| \quad (4)$$

3. Hybrid method

Full use of the available information - both time delay and power-attenuation - may be made by taking a weighted

sum of the above cost functions:

$$F_{u_i}(x, y, z, v, \alpha) = \sum_{j=1, j \neq i}^5 \left\{ K \cdot \left| \Delta P_{ij} - \left(\frac{r_j}{r_i} \right)^2 \cdot 10^{\alpha(r_i - r_j)} \right| + |r_j - r_i - \Delta T_{ij} \cdot v| \right\} \quad (5)$$

where K is a weighting factor. Various values of K could be used in the experiments.

4. Acoustic imaging method

Because of the likelihood that local minima of the cost functions could lead to false solutions, two approaches were previously used to estimate the variables x, y, z, v, and α [13]. A coarse search of the variable space, within predetermined limits, was made to narrow down the region where the true minimum occurs. Secondly the Nelder-Mead simplex search algorithm [14,15] was used to refine this search. In this algorithm, a simplex in n-dimensional space is characterized by the n+1 distinct vectors defining the vertices of the simplex. At each step of the search, a new point in or near the current simplex is generated. The function value at the new point is compared with the function values at the vertices of the simplex and the new point replaces one of the vertices if it has a low function value, giving a new simplex. This step is repeated until the diameter of the simplex is less than a specified tolerance. In both methods the value of the weighting factor, K, is not clearly defined.

In the present work, a new acoustic imaging method has been developed using the idea of the coarse searching approach. The procedure of the acoustic imaging for the passive sonar system is as follows. First of all, the variable space within predetermined limits is divided into smaller intervals. For example, $x = -250m, -245m, \dots, +245m, +250m$ with 5m interval in the x axis. Other variables, y, z, v and α , are also processed in the same way. Then two three-dimensional matrices, [A] and [B], are initialized. [A] matrix is assumed to contain x, y, z, v variables and [B] matrix is assumed to contain x, y, z, α variables. The sizes of [A] and [B] depends on the number of intervals in x, y, z dimensions. Then [A] matrix is filled with the cost function of the time-delay method with x, y, z, v variables. And [B] matrix is filled with the cost function of the power-attenuation method with x, y, z, α variables. Any element in [A] matrix contains the minimum cost function with regard to v variable, and any element in [B] matrix contains the minimum cost function with regard to α variable. After calculation both [A] and [B] are normalized. Because of this normalization the value of the weighting factor, K, is kept to be 1. That is, [A] and [B] matrices can be added together for each element of [A] and [B] resulting in a third matrix [C]. From given three-dimensional [C] matrix the element of the minimum cost function is searched. The searched minimum element actually indicates the estimated position of the acoustic source (x_i, y_i, z_i). Then since [C] matrix is three-dimensional, only x- and y- dimensional informations are extracted to form a two dimensional matrix [D] with (x, y, z_i). [D] is again normalized and multiplied with 256 for

visualization with 256 look-up color indices

IV. Results and discussion

The cartesian coordinates of the six hydrophones are listed in Table 1. The x- and y-coordinates are distances east and north respectively of a fixed reference point, while the z-coordinates are heights above mean sea level, determined from the known height of the ground surface and the depths of the boreholes. In practice there is some difficulty in determining precisely the x- and y-coordinates because of deviation from the vertical in the drilling operation. The hydrophone locations and hammering position are shown schematically in Fig. 3.

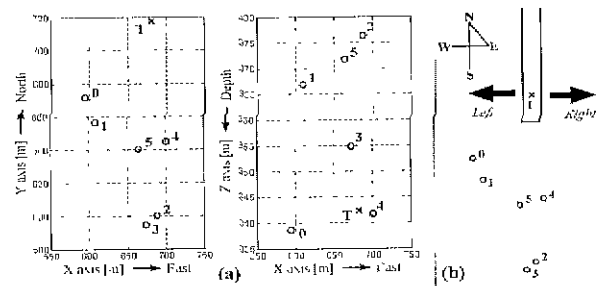


Fig. 3. Schematic views of hydrophone locations (o) and hammering position (x).

Table 1. Hydrophone locations and hammering position.

Sensor No.	x [m]	y [m]	z [m]	Distance from hammering position [m]
0	593.500	671.400	338.700	99.7646
1	608.700	656.400	366.800	98.3873
2	688.300	600.200	376.300	122.0842
3	673.600	594.200	354.900	124.0224
4	701.000	644.800	341.700	74.9491
5	664.100	640.300	371.700	84.3264
Hammer	682.004	717.299	342.348	

Typical time responses and their corresponding FFT spectra, for hydrophones, 0~5, are shown in Fig. 4 and 5 respectively. The time response for hydrophone 4 (the closest to the source) shows a clear second arrival of the hammering shock, believed to a reflection from the ground surface. Multiple paths may also result from refraction and scattering within the inhomogeneous medium, producing dispersion of the signal in time. This, together with environmental noise, leads to uncertainty in calculating time delays between the signals. Although the signals and their spectra are shown for the same hammering event, there are significant differences between the spectra, indicating that the attenuation is frequency-dependent.

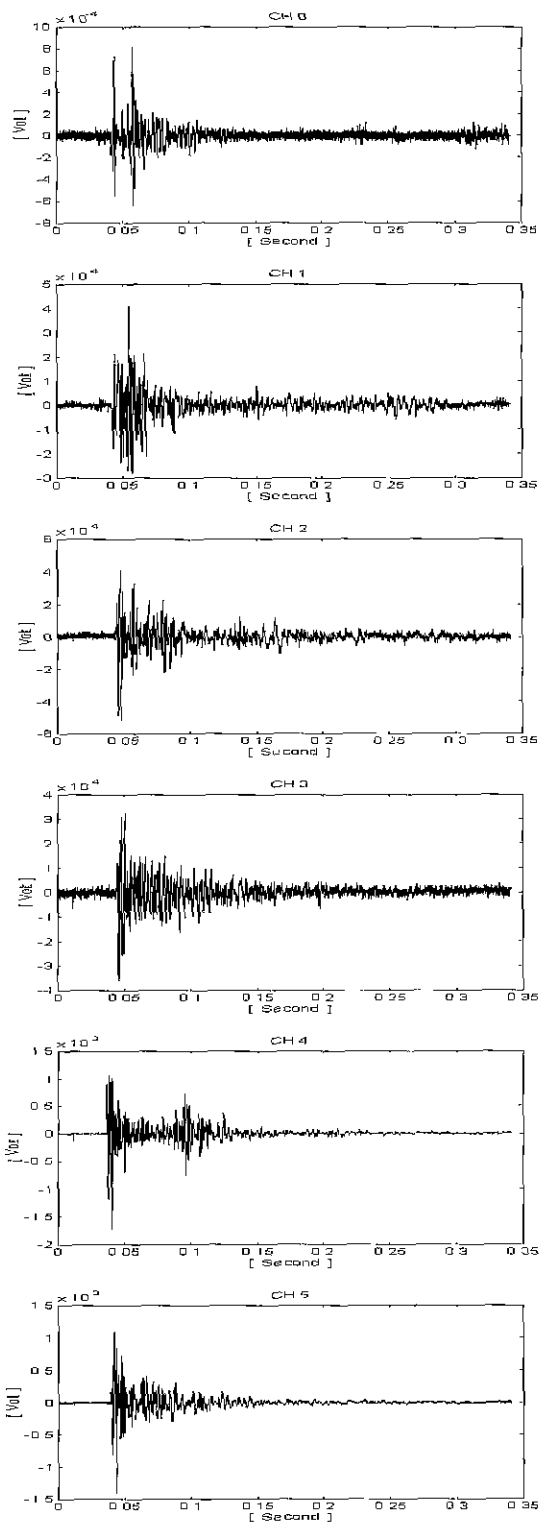


Fig. 4. Typical time responses of the hydrophones for a single hammer blow.

1. Time-delay method

The measured time delays between the hydrophone signals, calculated using cross correlation [16], are listed in Table 2. Because of the sampling frequency of 10 kHz, the values could be calculated only to the nearest 0.1 ms. Ideally the values should be anti-symmetric ($\Delta T_{ij} =$

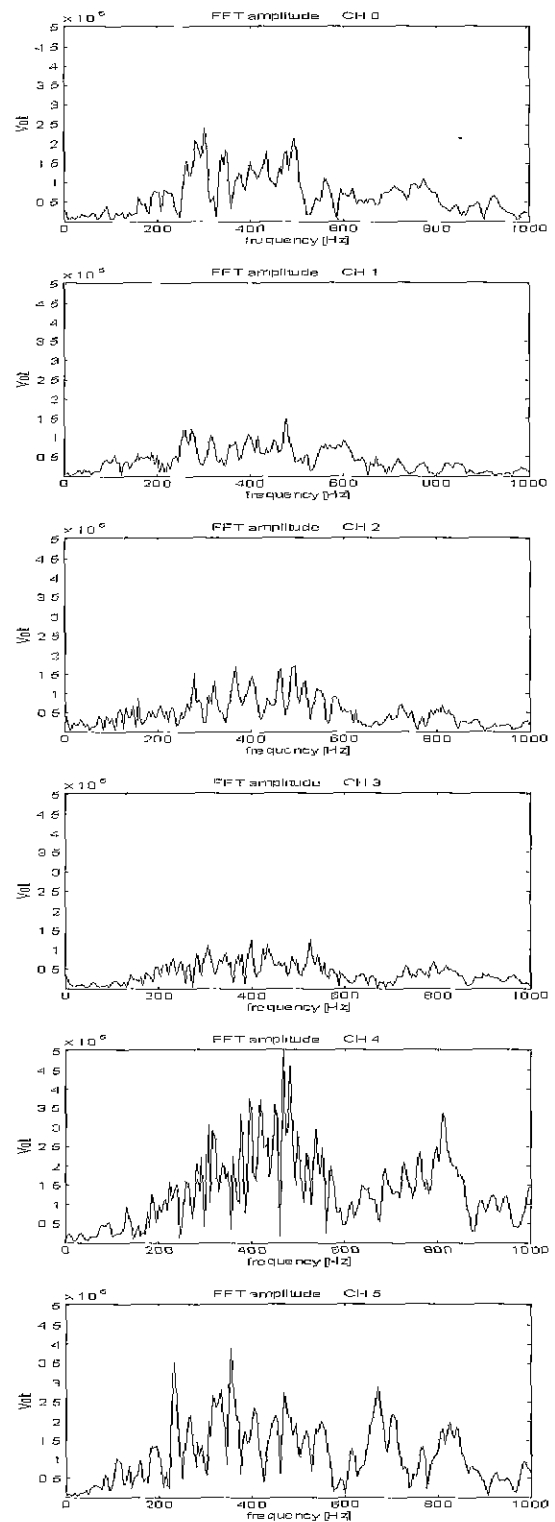


Fig. 5. FFT spectra of the time responses shown Fig. 4.

$-\Delta T_{ji}$) and related by the equation $\Delta T_{ij} = \Delta T_{ij} - \Delta T_{ji}$; however, deviation from this ideal occurs because of noise and propagation effects on the signals. For comparison, the theoretical time delays, calculated for the known source position and assumed velocity of sound $v=6000$ m/s, are shown in Table 3.

The estimates of the location of the sound source

obtained by minimising the time-delay function, matrix [A], are given to the nearest metre in Table 4. The estimates vary because of the emphasis that the time-delay function places on the reference hydrophone. In this experiment it is possible to compare the measured (Table 2) and theoretical time delays (Table 3) and from the differences to determine a measure of reliability for each hydrophone. However, this relies on knowing the true location of the source and so is not feasible in general.

Table 2. Measured time delays[ms] between hydrophones.

Obj. Ref.	0	1	2	3	4	5
0	0	0.2	4.3	4.4	-3.4	-1.2
1	-0.3	0	4.0	4.1	-4.2	-1.4
2	-4.3	-4.0	0	0.2	-8.1	-5.3
3	-4.4	-4.1	-0.1	0	-8.3	-5.5
4	3.4	4.3	8.0	8.2	0	2.8
5	1.2	1.4	5.2	5.5	-2.8	0

Table 3. Theoretical time delays [ms] for v = 6000 [m/s].

Obj. Ref.	0	1	2	3	4	5
0	0	0.23	3.72	4.04	-4.14	-2.70
1	-0.23	0	3.95	4.27	-3.91	-2.47
2	-3.72	-3.95	0	0.32	-7.86	-6.42
3	-4.04	-4.27	-0.32	0	-8.18	-6.74
4	4.14	3.91	7.86	8.18	0	1.44
5	2.70	2.47	6.42	6.74	-1.44	0

Table 4. Differences between estimated positions of the sound source and known location, distance errors $\sqrt{dx^2 + dy^2 + dz^2}$, and sound speed estimates using the time-delay method.

ref	dx [m]	dy [m]	dz [m]
0	3.9960	14.1010	-11.0480
1	-1.0040	-0.8990	-11.0480
2	13.9960	29.1010	-21.0480
3	8.9960	19.1010	-16.0480
4	18.9960	44.1010	-26.0480
5	18.9960	39.1010	-21.0480
Average	13.9960	34.1010	-21.0480
ref	Distance error from hammering position [m]	v [m/sec]	Value of Cost Function
0	18.3539	6600.0	2.953630
1	11.1299	6050.0	5.003430
2	38.5457	6500.0	3.698070
3	26.5201	6350.0	3.877470
4	54.6282	6650.0	1.135950
5	48.2986	6550.0	4.305480
Average	42.4474		

The values shown in the final column of Table 4 indicate that this provides a useful, if not infallible, guide - the lowest value of the time-delay function is that obtained when taking hydrophone 4 as the reference, and this may correspond to the best estimate. However, the correspondence is not universal, for example, using hydrophone 1 as reference produces a higher value of the cost function than in any other case but provides the best estimate of the location. The averaged value of the estimated locations with different references may therefore provide an assessment of the reliability of the measurements for each hydrophone. The averaged value of the estimated locations was not simply calculated in average from 6 estimated locations with regard to each of reference sensors. In that case any particular reference sensor could strongly affect the position estimation neglecting other reference sensors. The averaged value of Table 4 was in fact calculated from searching a minimum value of the summed elements of six [A] matrices where six [A] matrices were first calculated with every six reference sensors. By means of using all six normalized [A] matrices, the position estimation method can be equally affected from all six reference sensors. Since the averaged value of the estimated locations is calculated from 6 normalized [A] matrices, values of sound speed and cost function are meaningless in average.

2. Power-attenuation method

The measured power factors for each hydrophone, given by the right hand side of Eq. (3), are plotted in Fig. 6 (X) against distance from the known source location. Theoretical curves are also shown for a best-fit attenuation coefficient $\alpha=0.0164$ (continuous line) and for upper and lower bounds, $\alpha=0.0131$ and $\alpha=0.0205$ respectively (broken lines). The power ratios between the hydrophones, determined from the measured power factors, are listed in Table 5. Corresponding theoretical power ratios, calculated for $\alpha=0.0164$ and the known source location, are given in Table 6. The greatest discrepancy occurs in the values relating sensors 1 and 2, where the measured power ratio of sensor 2 relative to sensor 1 is over five times the theoretical ratio. This is also illustrated in Fig. 6, where the measured power factors for hydrophones 1 and 2 can be seen to lie at opposite extremes of the attenuation bounds. Further comparison of the measured and theoretical power ratios indicates that the discrepancy persists in all of the values with hydrophone 1 as the reference.

The solutions obtained for x, y, z, and α using the power-attenuation method are searched in matrix [B] and given in Table 7. The lowest value of the cost function occurs for reference hydrophone 4 and this corresponds to the worst estimate of position. The estimates of the source location are all similar although the values for reference hydrophones 2, 4 and 5 show considerable variation. The best estimate is that obtained with hydrophone 1 as reference. The averaged value of Table 7 was also calculated in the same way as that of Table 4.

3 Hybrid method

It may be expected that the hybrid method should give

Table 5. Measured power ratios (ΔP_{ij}) between hydrophones.

Obj. Ref.	0	1	2	3	4	5
0	1.0000	0.3842	0.5637	0.3320	4.1197	2.6409
1	2.6030	1.0000	1.4673	0.8643	10.7236	6.8744
2	1.7740	0.6815	1.0000	0.5890	7.3082	4.6849
3	3.0116	1.1570	1.6977	1.0000	12.4070	7.9535
4	0.2427	0.0933	0.1368	0.0806	1.0000	0.6410
5	0.3787	0.1455	0.2135	0.1257	1.5599	1.0000

Table 6. Theoretical power ratios for $\alpha=0.0164$ dB/m.

Obj. Ref.	0	1	2	3	4	5
0	1.0	1.08	0.288	0.259	4.52	2.51
1	0.923	1.0	0.266	0.239	4.17	2.31
2	3.47	3.76	1.0	0.901	15.7	8.70
3	3.857	4.18	1.11	1.0	17.4	9.66
4	0.221	0.240	0.064	0.057	1.0	0.555
5	0.399	0.432	0.115	0.104	1.80	1.0

Table 7. Differences between estimated positions of the sound source and known location, distance errors $\sqrt{dx^2 + dy^2 + dz^2}$, and attenuation estimates using the power-attenuation method.

ref	dx [m]	dy [m]	dz [m]
0	28.9960	49.1010	28.9520
1	18.9960	-25.8990	28.9520
2	38.9960	64.1010	38.9520
3	38.9960	59.1010	38.9520
4	38.9960	64.1010	38.9520
5	38.9960	64.1010	38.9520
Average	38.9960	64.1010	38.9520

ref	Distance error from hammering position [m]	α [dB/M]	Value of Cost Function
0	63.9523	1.5000E-2	0.904530
1	43.2415	1.2000E-2	2.519710
2	84.5392	1.6000E-2	1.605800
3	80.8138	1.6000E-2	2.812910
4	84.5392	1.6000E-2	0.214280
5	84.5392	1.6000E-2	0.334540
Average	84.5392		

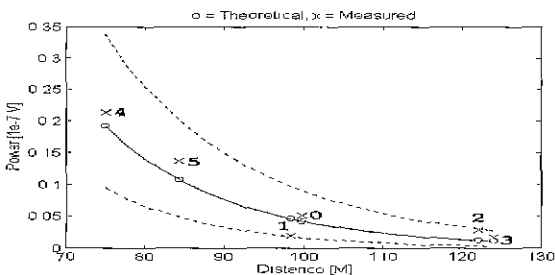


Fig. 6 Measured acoustic power (x) and theoretical power (o) of the hammering shock vs. distance.
 - Continuous line: $\alpha=0.0164$.
 - Broken lines: (upper) $\alpha=0.0131$, $\alpha=0.0205$.

intermediate values, improving the estimates of x, y and z. This is borne out in most cases by the estimates for the source location obtained from matrix [C] and shown in Table 8.

The finally averaged value of the estimated locations is calculated from 6 normalized [A] matrices and 6 normalized [B] matrices. The averaged value of the estimated location has 28m distance error. The results of Table 8 are the same as those of Table 4 with regard to each of reference sensors except the averaged values. That is, the averaged value of Table 8 shows better results than that of Table 4. This means that the time-delay information is more strongly affects for the position estimation than the power-attenuation method. Also the hybrid method produces the best position estimation because the hybrid method uses both time-delay and power-attenuation informations. Fig. 7 shows the matrix [D] in a colorful imaged pattern. The acoustic imaging method certainly shows the multi-dimensional distribution of the normalized cost function, so as to indicate the trend of the minimizing direction toward the source location.

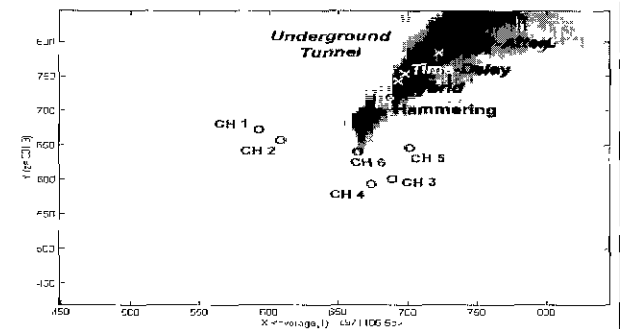


Fig. 7. The acoustic imaging pattern of matrix [D] derived as explained in acoustic imaging method.

Table 8. Differences between estimated positions of the sound source and known location, distance errors using $\sqrt{dx^2 + dy^2 + dz^2}$ the hybrid method.

ref	dx [m]	dy [m]	dz [m]	Distance error from hammering position [m]
0	3.9960	14.1010	-11.0480	18.3539
1	-1.0040	-0.8990	-11.0480	11.1299
2	13.9960	29.1010	-21.0480	38.5457
3	8.9960	19.1010	-16.0480	26.5201
4	18.9960	44.1010	-26.0480	54.6282
5	18.9960	39.1010	-21.0480	48.2986
Average	8.9960	24.1010	-11.0480	27.9972

V. Conclusions

Three methods for estimating the location of an underground sound source using measurements from an array of hydrophones have been presented. In the experiment reported, where the source was on one side of the array, the time-delay method gave better estimated locations than the power-attenuation method. The hybrid method is capable of steering a middle path to give more accurate

estimates. Of the three methods, the power-attenuation method was the slowest to converge. This new acoustic imaging method can be practically used to verify any algorithm of faster searching for the position of the source for the next work.

Various matters remain to be addressed. All of the methods rely on the choice of a reference hydrophone; some attempt has been made to assess the reliability of the information provided by each hydrophone but this work needs to be extended to enable the choice to be made without prior knowledge of the location of the source. Alternatively the methods could be recast to be independent of such a choice.

The experimental data could be improved by using higher sampling rates in recording the time signals and by using statistical averaging over a number of detections of sound from the sound source

In the experiment reported the hydrophone sensitivity is sufficient to record the hammering shock up to a range of at least 250 m and the results suggest that an estimation of location can be made to within 28 m. The use of geophones in the suspected area may then be a feasible approach to determine the location more accurately [2,3].

Other features of the problem are more difficult to address. The assumption of uniform sound propagation velocity and attenuation coefficient is open to question and could be improved only with prior knowledge of the underground medium. Other propagation phenomena - reflection, reverberation, scattering, refraction - also need to be taken into account.

References

- [1] R. F. Ballard, *Tunnel Detection*, U.S. Army Engineer Waterways Experiment Station, Technical Report GL-82-9, 1982.
- [2] R. J. Greenfield, *Seismic Analysis of Tunnel Boring Machines Signals at Kerckhoff Tunnel*, U.S. Army Engineer Waterways Experiment Station, Miscellaneous Paper GL-83-19, 1983.
- [3] R. J. Greenfield, *The WES Seismic Listening System (SLS)*, reported by U.S. Army Engineer Waterways Experiment Station, Vicksburg, Mississippi, 1987.
- [4] D. Stansfield, *Underwater Electroacoustic Transducers*, Bath University Press and Institute of Acoustics, pp. 300, 1990.
- [5] *Acoustic Emission Testing*, ASNT (American Society of Non-destructive Testing) Handbook. 2nd Edition, 5, pp. 314, 1991.
- [6] R. F. W. Coates, *Underwater Acoustic Systems*, Macmillan Education Ltd. 1990.
- [7] *Sound & Vibration Product Catalogue*. Brüel and Kjær, 1995.
- [8] P. Horowitz and W. Hill, *The Art of Electronics*, Cambridge University Press, Cambridge, pp. 457-466, 1990.
- [9] S. S. Jarng, J. A. Park, and K. H. Rhee, "Development of underground acoustic noise rejection method," *Basic Science and Eng.*, The Int. J. of Chosun Uni., 1(2), pp. 1035-1041, 1997.
- [10] *Data Acquisition with DT VEE*, Data Translation U.S.A., 1995.
- [11] J. S. Bendat and A. G. Piersol, *Random Data Analysis and Measurement Procedures*, John Wiley and Sons, pp. 332, 1971.
- [12] A. Ben-Menahem and S. J. Singh, *Seismic Waves and Sources*, Springer-Verlag, p. 1056, 1981.
- [13] S. S. Jarng, J. H. Lee and D. T. I. Francis, "Development of a passive sonar system for localisation of an underground acoustic source," *Proceedings of the Institute of Acoustics*, 20, Pt 7, pp. 147-156, 1998.
- [14] J. A. Nelder and R. Mead, *A simplex method for function minimization*, *Computer Journal*, 7, pp. 308-313, 1965.
- [15] J. E. Dennis Jr. and D. J. Woods, *New computing environments microcomputers in large-scale computing*, edited by A. Wouk. SIAM, pp. 116-122, 1987.
- [16] A. V. Oppenheim and R. W. Schaffer, *Digital Signal Processing*. Prentice-Hall, pp. 539, 1975.



Soon Suck Jarng

B. Eng. in Electronics at HanYang Uni.(1984), M. Eng. in Electronics at Hull Uni.(1985), M. Sc. in Physiology at Birmingham Uni.(1988), Ph.D. in Electronic & Electrical Eng at Birmingham Uni.(1991). Currently, Professor in Control & Inst. at Chosun Uni. The interested parts are sonar, acoustic, medical-eng, fem, bem, sensor design, etc.



Heung Gu Ahn

B. Eng. in Control & Inst. at Chosun Uni. (1999). Currently, M. Eng. in Control & Inst. at Chosun Uni. The interested parts are acoustic, position estimation, fem, bem, sensor, etc.



Je Hyeong Lee

B. Eng. in Control & Inst. at Chosun Uni. (1997), M. Eng. in Control & Inst. at Chosun Uni. (1999). Currently, Ph.D in Control & Inst. at Chosun Uni. The interested parts are acoustic, fem, bem, sensor, etc.